Iranian Journal of Science and Technology, Transactions of Mechanical Engineering (2022) 46:649–665
https://doi.org/10.1007/s40997-021-00429-1

RESEARCH PAPER

Nonlinear Forced Vibration and Dynamic Buckling Analysis for Functionally Graded Cylindrical Shells with Variable Thickness Subjected to Mechanical Load

K. V. Phu[1] · D. H. Bich[1] · L. X. Doan[2]

Received: 21 November 2020 / Accepted: 7 March 2021 / Published online: 24 March 2021

Abstract
This paper presents the analytical approach to investigate the nonlinear forced vibration and dynamic buckling of the variable thickness functionally graded cylindrical shells subjected to mechanical load. The nonlinear motion equations of FGM cylindrical shell with variable thickness based on classical shell theory and von Kármán geometric nonlinearity are derived. The Galerkin method and the fourth-order Runge–Kutta method are applied to solve the governing equations of dynamic system. The effects of material (coefficient k) and geometric parameters on the nonlinear forced vibration and dynamic buckling behavior of the FG shell with variable thickness are examined in detail.

Keywords Nonlinear forced vibration · Dynamic buckling · Variable thickness · FGM cylindrical shell · Dynamic responses

1 Introduction

Structures made of the FG material are special structures and widely used in life such as construction industry, mechanical structures, air transport or a nuclear reactor. Variable thickness FGM shell helps to reduce the weight of structure and saves materials while ensuring load capacity; therefore, it is more and more popularly used in important industries. Study on nonlinear vibration and stability of FGM shell with variable thickness is necessary to make sure the structure works efficiently and reliably.

The nonlinear vibration and dynamic stability of FGM shell structure have been analyzed by several scientists. For instance, Loy et al. (1999, 2000) studied the natural frequencies of FG cylindrical shell subjected to mechanical load. Some influences of factors on natural frequencies of the structure were also examined. Sofiyev et al. (2003, 2013) presented nonlinear dynamic buckling analysis of FGM cylindrical and truncated conical shell subjected to impulsive and axial compressive load by using analytical method based on Love's shell theory. Haddadpour et al. (2007), based on the Love shell theory and Galerkin method, investigated the free vibration of simply supported FGM circular cylinder shell with four different boundary conditions, and the nonlinear geometries of von Karman were taken into account. Matsunaga (2009) presented the vibration and stability analysis of FGM circular cylinder shell subjected to mechanical load based on the two-dimensional higher-order shear deformation theory (HSDT). Hamilton's principle and power series expansion method were used to build the governing equation in this work. Bich and Nguyen (2012) based on improved Donnell shell theory and Volmir's assumption to analyze the nonlinear vibration of FGM cylindrical shell subjected to mechanical load. The Galerkin method and the fourth-order Runge–Kutta method were employed to survey influences of FG material features, pre-loaded axial compression and dimensional ratios on the dynamical response of shells. Also based on the same theory, Avramov (2011) used the Galerkin method and harmonic balance method to study nonlinear vibration and stability of simply supported FGM cylindrical shells. Duc et al. (2014, 2015, 2014, 2015, 2016) studied nonlinear vibration, buckling and post-buckling of eccentrically stiffened S-FGM circular cylindrical shells surrounded by

✉ L. X. Doan
xuandoan1085@tdnu.edu.vn

[1] Vietnam National University, 144 Xuan Thuy – Cau Giay, Hanoi, Vietnam

[2] Tran Dai Nghia University, 189 Nguyen Oanh- Go Vap, Ho Chi Minh City, Vietnam

elastic foundations subjected to mechanical load in thermal environments. The Lekhnitsky's smeared stiffener technique, the stress function and Galerkin method are employed to solve these problems. Wann (2015,) based on the first-order shear deformation theory (FSDT), Rayleigh Ritz method and variational approach, investigated the free vibration of FGM cylinder shells resting on the Pasternak elastic medium by using the analytical method. Malekzadeh et al. (2013) investigated the free vibration of rotating FGM truncated conical shells subjected to mechanical load with various boundary conditions. Dynamic equilibrium equations and motion equations of the shell were derived according to the FSDT. Nonlinear dynamic problems of imperfect double-curved shallow shells made of FGM and surrounded by elastic foundations have been solved by Duc et al. (2013, 2016). In this study, natural frequencies of the structures are calculated by using shear deformation shell theories, the Galerkin method and the fourth-order Runge–Kutta method. Also by using analytical method, nonlinear dynamics problem of cylindrical panels made of FGM and S-FGM has been solved by Quan et al. (2014, 2015). Alibeigloo et al. (2017) replied on elastic theories and differential quadrature method (DQM) to study the free vibration of simply supported sandwich FGM cylindrical shells. Using an analytical approach, Thanh et al. (2019) solved the nonlinear dynamic problems of imperfect FGM reinforced by carbon nanotube by using the Reddy's FSDT, the Galerkin method and the fourth-order Runge–Kutta method. Also using analytical method, Phu et al. (2017, 2019) studied the nonlinear vibration of sandwich FGM and stiffened sandwich FGM cylindrical shell filled with fluid subjected to mechanical loads in thermal environment. The classical shell theory with geometrical nonlinearity in von Karman–Donnell sense and smeared stiffener technique were used to define motion equations of structure. Natural frequencies and dynamic responses of the shell were determined by using Galerkin's method and Runge–Kutta method. By using the same approach, Dat et al. (2019) studied the nonlinear vibration of FGM elliptical cylindrical shells reinforced by carbon nanotube resting on elastic foundation subjected to thermal–mechanical load. Han et al. (2018) predicted free vibration of FGM thin cylinder shells filled inside with pressurized fluid based on Flügge shell theory. In governing equations, internal static pressure was regarded as the pre-stress term. On dynamic stability analysis of FGM shell, Huang et al. (2008, 2010a; b) solved nonlinear dynamic buckling problems of FGM cylindrical shells subjected to mechanical load based on Donnell shell theory and large deflection theory. Nonlinear dynamic responses of structure were obtained by applying energy method and the four-order Runge–Kutta method. The critical loads were determined according to Budiansky–Roth criterion. By the same method, Dung et al. (2015, 2017) focused on solving nonlinear dynamic buckling problems of stiffened FGM thin cylindrical shells surrounded by elastic foundations subjected to mechanical load in thermal environments. Recently, Zhang et al. (2019) focused on solving on dynamic buckling of FGM cylindrical shells under thermal shock based on the Hamiltonian principle. Nonlinear torsional buckling problems of sandwich FGM cylindrical shells with spiral stiffeners under torsion and thermal loads were solved by Nam et al. (2019).

Recently, there are some scientists interested in static and dynamic problems of variable thickness FGM cylindrical shell; for example, Sofiyev AH et al. (2002) analyzed dynamic buckling of variable thickness elastic cylindrical shell subjected to external pressure. The critical static and dynamics loads of the structure were found by using Galerkin's method and Ritz method. Ghannad et al. (2017, 2019) solved thermo-elastic problems of FGM cylindrical shells with variable thickness subjected to thermal–mechanical loads based on shear deformation theories. The distribution of displacement and stress in axial and radial direction were determined by using matched asymptotic method and finite element method (FEM). Selah et al. (2014) studied the mechanical responses of the variable thickness FGM truncated conical shell under asymmetric pressure using three dimensions elasticity theory and DQM. Using a semi-analytical approach based on the HSDT and multi-layer method, Jabbari and his co-workers examined thermo-elastic responses of FGM thick cylindrical Shell (2015) and truncated conical shell (2016) with the variable thickness subjected to thermal–mechanical load. Also, Kashkoli et al. (2018) studied the thermo-mechanical creep of thick variable thickness FGM-cylindrical pressure vessel under thermal–mechanical load. Shariyat et al. (2017) presented an investigation of the stresses and displacements of the variable thickness FGM cylindrical and truncated conical shells with different boundary conditions by using the FSDT. By using the Generalized DQM, the free vibration problems of singly-curved and doubly curved laminated composite shells with variable thickness were solved by Bacciocchi et al. (2016). Shariyat and Asgari (2013) used FEM replied on the third-order shear deformation theory and modified Budiansky's criterion to present an analysis for thermal buckling and post-buckling of imperfect cylindrical shells with variable thickness made of bidirectional FGM.

According to the above reviews and the best author's knowledge, the nonlinear forced vibration and dynamic buckling behavior of variable thickness FGM cylindrical shells subjected to mechanical load are investigated for the first time. In the present article, by using the analytical approach based on the classical shell theory and von Kármán geometric nonlinearity, the governing equation of the variable thickness FGM cylindrical shell is derived. The obtained results of the present study are compared with other published works to demonstrate the accuracy and reliability of the present proposed method. Furthermore, the effects of the material, geometric parameters on responses of the structure are examined in detail.

2 Governing Equations

Consider a variable thickness FGM cylindrical shell with the length L and the radius R subjected to uniform external pressure $q(t)$ and axial compression load $p(t)$ (Fig. 1). Assume that the radius of shell are much larger than the thickness ($R >> h$), thickness of the shell h can be determined as: $h_{(x)} = ax + b$.

in which $a = (h_1 - h_0)/L$; $b = h_0$.

The effective properties of material can be expressed as follows:

$$P(z) = P_{\mathrm{m}} \cdot V_{\mathrm{m}}(z) + P_c \cdot V_c(z) = P_{\mathrm{m}} + \left(P_c - P_m\right)V_c(z) \quad (1)$$

in which P_m and P_c are material and ceramic properties, V_c and V_m are volume fractions of ceramic and metal constituent, respectively, and are related by $V_c + V_m = 1$.

Ceramic volume fractions in the structure are distributed as following law:

$$\mathrm{V_c}(z) = \left(\frac{1}{2} + \frac{z}{h_{(x)}}\right)^k \quad (2)$$

Poisson's ratio is assumed to be constant ($\nu = constant$).

According to the classical shell theory (Brush et al. 1975, Duc ND 2014) the strain–displacement relationship of the shells:

$$\varepsilon_{ij} = \varepsilon_{ij}^0 + zk_{ij}\, with\, (ij = xx,\ yy,\ xy) \quad (3)$$

in which

Applying Hooke's law for the FGM shell subjected to mechanical load:

$$\begin{Bmatrix} \sigma_{xx} \\ \sigma_{yy} \\ \tau_{xy} \end{Bmatrix} = \frac{E_{(z)}}{1 - \upsilon_{(z)}^2} \begin{bmatrix} 1 & \nu & 0 \\ \nu & 1 & 0 \\ 0 & 0 & (1-\nu)/2 \end{bmatrix} \cdot \begin{Bmatrix} \varepsilon_{xx} \\ \varepsilon_{yy} \\ \gamma_{xy} \end{Bmatrix} or\, \{\sigma\} = [\Pi] \cdot \{\varepsilon\} \quad (5)$$

Integrating Stress–Strain relationship through the thickness of the shell, we obtain the governing equations of the variable thickness FGM cylindrical shell:

$$\left\{ \begin{matrix} \{N_{ij}\} \\ \{M_{ij}\} \end{matrix} \right\} = \begin{bmatrix} [A] & [B] \\ [B] & [D] \end{bmatrix} \cdot \left\{ \begin{matrix} \{\varepsilon_{ij}^0\} \\ \{k_{ij}\} \end{matrix} \right\} \text{with}\, (i,j) = (xx\,, yy,\, xy) \quad (6)$$

in which

$$\{[A];[B];[D]\} = \int_{-h_{(x)}/2}^{h_{(x)}/2} [\Pi].\left(1, z, z^2\right) dz \quad (7)$$

Equation (6) can be rewritten as follows:

$$\begin{Bmatrix} N_{xx} \\ N_{yy} \\ N_{xy} \\ M_{xx} \\ M_{yy} \\ M_{xy} \end{Bmatrix} = \begin{bmatrix} A_{11} & A_{12} & 0 & B_{11} & B_{12} & 0 \\ A_{21} & A_{22} & 0 & B_{21} & B_{22} & 0 \\ 0 & 0 & A_{66} & 0 & 0 & B_{66} \\ B_{11} & B_{12} & 0 & D_{11} & D_{12} & 0 \\ B_{21} & B_{22} & 0 & D_{21} & D_{22} & 0 \\ 0 & 0 & B_{66} & 0 & 0 & D_{66} \end{bmatrix} \cdot \begin{Bmatrix} \varepsilon_{xx}^0 \\ \varepsilon_{yy}^0 \\ \gamma_{xy}^0 \\ k_{xx} \\ k_{yy} \\ k_{xy} \end{Bmatrix} \quad (8)$$

in which

$$\begin{cases} \varepsilon_{xx}^0 = \dfrac{\partial u_0}{\partial x} + \dfrac{1}{2}\left(\dfrac{\partial w}{\partial x}\right)^2 ; \varepsilon_{yy}^0 = \dfrac{\partial v_0}{\partial y} - \dfrac{w}{R} + \dfrac{1}{2}\left(\dfrac{\partial w}{\partial y}\right)^2 ; \gamma_{xy}^0 = \dfrac{\partial u_0}{\partial y} + \dfrac{\partial v_0}{\partial x} + \dfrac{\partial w}{\partial x}\dfrac{\partial w}{\partial y} \\ k_{xx} = -\dfrac{\partial^2 w}{\partial x^2} ; k_{yy} = -\dfrac{\partial^2 w}{\partial y^2} ; k_{xy} = -2\dfrac{\partial^2 w}{\partial x \partial y} \end{cases} \quad (4)$$

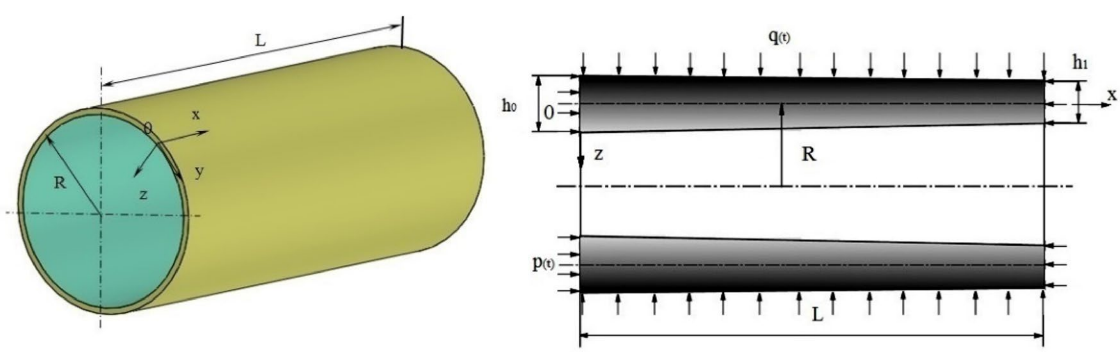

Fig. 1 Variable thickness FGM cylindrical shell

$$A_{11}=A_{22}=\frac{E_1\cdot h_{(x)}}{1-\nu^2};A_{12}=A_{21}=\frac{\nu\cdot E_1\cdot h_{(x)}}{1-\nu^2};B_{11}=B_{22}=\frac{E_2\cdot h^2_{(x)}}{1-\nu^2};B_{12}=B_{21}=\frac{\nu\cdot E_2\cdot h^2_{(x)}}{1-\nu^2};$$

$$D_{11}=D_{22}=\frac{E_3\cdot h^3_{(x)}}{1-\nu^2};D_{12}=D_{21}=\frac{\nu\cdot E_3\cdot h^3_{(x)}}{1-\nu^2};A_{66}==\frac{E_1\cdot h_{(x)}}{2(1+\nu)};B_{66}=\frac{E_2\cdot h^2_{(x)}}{2(1+\nu)};D_{66}=\frac{E_2\cdot h^2_{(x)}}{2(1+\nu)}$$

with:

$$E_1=E_{\mathrm{m}}+\frac{E_{\mathrm{c}}-E_{\mathrm{m}}}{(k+1)};E_2=\frac{\left(E_{\mathrm{c}}-E_{\mathrm{m}}\right)k}{2(k+1)(k+2)};E_3=\frac{E_{\mathrm{m}}}{12}+\left(E_c-E_{\mathrm{m}}\right)\left(\frac{1}{k+3}-\frac{1}{k+2}+\frac{1}{4(k+1)}\right).$$

Internal force and moment resultants can be obtained from Eq. (7) as follows:

$$\begin{cases}N_{xx}=A_{11}\left(\varepsilon^0_{xx}+\upsilon\cdot\varepsilon^0_{yy}\right)+B_{11}\left(k_{xx}+\nu\cdot k_{yy}\right)\\ N_{yy}=A_{11}\left(\varepsilon^0_{yy}+\upsilon\cdot\varepsilon^0_{xx}\right)+B_{11}\left(k_{yy}+\nu\cdot k_{xx}\right)\\ N_{xy}=A_{66}\cdot\gamma^0_{xy}+B_{66}\cdot k_{xy}\\ M_{xx}=B_{11}\left(\varepsilon^0_{xx}+\nu\cdot\varepsilon^0_{yy}\right)+D_{11}\left(k_{xx}+\nu\cdot k_{yy}\right)\\ M_{yy}=B_{11}\left(\varepsilon^0_{yy}+\nu\cdot\varepsilon^0_{xx}\right)+D_{11}\left(k_{yy}+\nu\cdot k_{xx}\right)\\ M_{xy}=B_{66}\cdot\gamma^0_{xy}+D_{66}\cdot k_{xy}\end{cases}\tag{9}$$

Nonlinear motion equations of FGM cylindrical shell with variable thickness based on classical shell theory (Brush et al. 1975) are:

$$\begin{cases}\dfrac{\partial N_{\mathrm{xx}}}{\partial x}+\dfrac{\partial N_{\mathrm{xy}}}{\partial y}=\rho_1\dfrac{\partial^2 u}{\partial t^2}\\ \dfrac{\partial N_{xy}}{\partial x}+\dfrac{\partial N_{yy}}{\partial y}=\rho_1\dfrac{\partial^2 v}{\partial t^2}\\ \dfrac{\partial^2 M_{xx}}{\partial x^2}+2\dfrac{\partial^2 M_{xy}}{\partial x\partial y}+\dfrac{\partial^2 M_{yy}}{\partial y^2}\\ +N_{xx}\cdot\dfrac{\partial^2 w}{\partial x^2}+2N_{xy}\dfrac{\partial^2 w}{\partial x\partial y}+N_{yy}\dfrac{\partial^2 w}{\partial y^2}\\ +\dfrac{N_y}{R}-p\cdot h(x)\dfrac{\partial^2 w}{\partial x^2}+q=\rho_1\dfrac{\partial^2 w}{\partial t^2}+2\varepsilon\rho_1\dfrac{\partial w}{\partial t}\end{cases}\tag{10}$$

in which $\rho_1=\left(\rho_m+\frac{\rho_c-\rho_m}{k+1}\right)h_{(x)}=\rho^*_1 h_{(x)}$

Substituting Eq. (3) and Eq. in Eq. (10), we obtain:

$$\begin{cases}L_{11}(u)+L_{12}(v)+L_{13}(w)+P_1(w)=\rho_1\dfrac{\partial^2 u}{\partial t^2}\\ L_{21}(u)+L_{22}(v)+L_{23}(w)+P_2(w)=\rho_1\dfrac{\partial^2 v}{\partial t^2}\\ L_{31}(u)+L_{32}(v)+L_{33}(w)+P_3(w)+P_4(u,w)+P_5(v,w)+q+p.h(x,y)\dfrac{\partial^2 w}{\partial x^2}=\rho_1\dfrac{\partial^2 w}{\partial t^2}+2\varepsilon\rho_1\dfrac{\partial w}{\partial t}\end{cases}\tag{11}$$

in which

$$L_{11}(u)=A_{11}\frac{\partial^2 u}{\partial x^2}+\frac{\partial A_{11}}{\partial x}\frac{\partial u}{\partial x}+A_{66}\cdot\frac{\partial^2 u}{\partial y^2};L_{12}(v)=A_{66}\cdot\frac{\partial^2 v}{\partial x\partial y}+\nu\cdot\frac{\partial A_{11}}{\partial x}\frac{\partial v}{\partial y}+\nu\cdot A_{11}\frac{\partial^2 v}{\partial x\partial y}$$

$$L_{13}(w) = -B_{11}\frac{\partial^3 w}{\partial x^3} - \nu \cdot B_{11}\frac{\partial^3 w}{\partial x \partial y^2} - 2B_{66}\cdot\frac{\partial^3 w}{\partial x \partial y^2} - \frac{\partial B_{11}}{\partial x}\frac{\partial^2 w}{\partial x^2} - \nu\cdot\frac{\partial B_{11}}{\partial x}\frac{\partial^2 w}{\partial y^2} - \nu\cdot\frac{\partial A_{11}}{\partial x}\frac{w}{R} - \frac{1}{R}\nu\cdot A_{11}\frac{\partial w}{\partial x};$$

$$P_1(\mathrm{w}) = \frac{1}{2}\frac{\partial A_{11}}{\partial x}\left(\left(\frac{\partial w}{\partial x}\right)^2 + \nu.\left(\frac{\partial w}{\partial y}\right)^2\right) + A_{11}\left(\frac{\partial w}{\partial x}\frac{\partial^2 w}{\partial x^2} + \nu.\frac{\partial w}{\partial y}\frac{\partial^2 w}{\partial x \partial y}\right) + A_{66}.\left(\frac{\partial^2 w}{\partial x \partial y}\frac{\partial w}{\partial y} + \frac{\partial w}{\partial x}\frac{\partial^2 w}{\partial y^2}\right);$$

$$L_{21}(u) = \left(A_{66} + A_{11}\nu\right).\frac{\partial^2 u}{\partial x \partial y} + \frac{\partial A_{66}}{\partial x}\frac{\partial u}{\partial y}; L_{22}(v) = A_{66}.\frac{\partial^2 \mathrm{v}}{\partial x^2} + \frac{\partial A_{66}}{\partial x}\frac{\partial \mathrm{v}}{\partial x} + A_{11}\frac{\partial^2 \mathrm{v}}{\partial y^2};$$

$$L_{23}(w) = -B_{11}\frac{\partial^3 w}{\partial y^3} - \left(\nu B_{11} + 2B_{66}\right)\cdot\frac{\partial^3 w}{\partial x^2 \partial y} - 2\frac{\partial B_{66}}{\partial x}\cdot\frac{\partial^2 w}{\partial x \partial y} - \frac{1}{R}A_{11}\frac{\partial w}{\partial y};$$

$$P_2(w) = A_{11}\left(\frac{\partial w}{\partial y}\frac{\partial^2 w}{\partial y^2} + \nu\frac{\partial w}{\partial x}\frac{\partial^2 w}{\partial x \partial y}\right) + A_{66}\cdot\frac{\partial^2 w}{\partial x^2}\frac{\partial w}{\partial y} + A_{66}\cdot\frac{\partial w}{\partial x}\frac{\partial^2 w}{\partial x \partial y} + \frac{\partial A_{66}}{\partial x}\frac{\partial w}{\partial x}\frac{\partial w}{\partial y};$$

$$I_{31}(u) = B_{11}\frac{\partial^3 u}{\partial x^3} + \left(2B_{66} + \nu\cdot B_{11}\right)\frac{\partial^3 u}{\partial x \partial y^2} + 2\frac{\partial B_{11}}{\partial x}\frac{\partial^2 u}{\partial x^2} + \frac{\partial^2 B_{11}}{\partial x^2}\frac{\partial u}{\partial x} + 2\frac{\partial B_{66}}{\partial x}\frac{\partial^2 u}{\partial y^2} + \frac{1}{R}\nu\cdot A_{11}\frac{\partial u}{\partial x};$$

$$L_{32}(v) = B_{11}\frac{\partial^3 v}{\partial y^3} + \left(2B_{66} + \nu\cdot B_{11}\right)\frac{\partial^3 v}{\partial x^2 \partial y} + 2\nu\cdot\frac{\partial B_{11}}{\partial x}\frac{\partial^2 v}{\partial x \partial y} + 2\frac{\partial B_{66}}{\partial x}\frac{\partial^2 v}{\partial x \partial y} + \nu\frac{\partial^2 B_{11}}{\partial x^2}\frac{\partial v}{\partial y} + \frac{1}{R}A_{11}\frac{\partial v}{\partial y};$$

$$\begin{aligned} L_{33}(w) = &- D_{11}\left(\frac{\partial^4 w}{\partial x^4} + \frac{\partial^4 w}{\partial y^4}\right) - 2\left(D_{11}\nu + 2D_{66}\right)\frac{\partial^4 w}{\partial x^2 \partial y^2} - 2\frac{\partial D_{11}}{\partial x}\left(\frac{\partial^3 w}{\partial x^3} + \nu\cdot\frac{\partial^3 w}{\partial x^2 \partial y}\right) - \frac{\partial^2 D_{11}}{\partial x^2}\left(\frac{\partial^2 w}{\partial x^2} - \nu\cdot\frac{\partial^2 w}{\partial y^2}\right) \\ &- \nu\cdot\frac{\partial^2 B_{11}}{\partial x^2}\frac{w}{R} - \frac{1}{R}A_{11}\frac{w}{R} - \frac{2}{R}\nu\cdot\frac{\partial B_{11}}{\partial x}\frac{\partial w}{\partial x} - \frac{2}{R}\nu\cdot B_{11}\frac{\partial^2 w}{\partial x^2} - \frac{2}{R}B_{11}\frac{\partial^2 w}{\partial y^2} - 4\frac{\partial D_{66}}{\partial x}\cdot\frac{\partial^3 w}{\partial x \partial y^2}; \end{aligned}$$

$$\begin{aligned} P_3(w) = &\frac{1}{2R}A_{11}\left(\left(\frac{\partial w}{\partial y}\right)^2 + \nu\cdot\left(\frac{\partial w}{\partial x}\right)^2\right) - A_{11}\frac{w}{R}\left(\frac{\partial^2 w}{\partial y^2} - \nu\cdot\frac{\partial^2 w}{\partial x^2}\right) + \frac{1}{2}\frac{\partial^2 B_{11}}{\partial x^2}\left(\left(\frac{\partial w}{\partial x}\right)^2 + \nu\cdot\left(\frac{\partial w}{\partial y}\right)^2\right) \\ &+ 2\frac{\partial B_{11}}{\partial x}\left(\frac{\partial w}{\partial x}\frac{\partial^2 w}{\partial x^2} + \nu\cdot\frac{\partial w}{\partial y}\frac{\partial^2 w}{\partial x \partial y}\right) + B_{11}\left(2\nu\cdot\left(\frac{\partial^2 w}{\partial x \partial y}\right)^2 + \frac{\partial w}{\partial y}\frac{\partial^3 w}{\partial y^3} + \frac{\partial w}{\partial x}\frac{\partial^3 w}{\partial x^3} + \nu\cdot\frac{\partial w}{\partial y}\frac{\partial^3 w}{\partial x^2 \partial y} + \nu\frac{\partial w}{\partial x}\frac{\partial^3 w}{\partial x \partial y^2}\right) \\ &- 2B_{11}\nu\frac{\partial^2 w}{\partial y^2}\frac{\partial^2 w}{\partial x^2} + 2\frac{\partial B_{66}}{\partial x}\left(\frac{\partial^2 w}{\partial x \partial y}\frac{\partial w}{\partial y} + \frac{\partial w}{\partial x}\frac{\partial^2 w}{\partial y^2}\right) + 2B_{66}.\left(\frac{\partial^3 w}{\partial x^2 \partial y}\frac{\partial w}{\partial y} + \frac{\partial^2 w}{\partial x^2}\frac{\partial^2 w}{\partial y^2} - \left(\frac{\partial^2 w}{\partial x \partial y}\right)^2 + \frac{\partial w}{\partial x}\frac{\partial^3 w}{\partial x \partial y^2}\right); \end{aligned}$$

$$P_4(w) = \frac{1}{2}A_{11}\frac{\partial^2 w}{\partial x^2}\left(\left(\frac{\partial w}{\partial x}\right)^2 + \nu\cdot\left(\frac{\partial w}{\partial y}\right)^2\right) + \frac{1}{2}A_{11}\frac{\partial^2 w}{\partial y^2}\left(\left(\frac{\partial w}{\partial y}\right)^2 + \nu.\left(\frac{\partial w}{\partial x}\right)^2\right) + 2A_{66}\cdot\frac{\partial w}{\partial x}\frac{\partial w}{\partial y}\frac{\partial^2 w}{\partial x \partial y};$$

$$P_5(u,w) = A_{11}\frac{\partial u}{\partial x}\frac{\partial^2 w}{\partial x^2} + \nu\cdot A_{11}\frac{\partial u}{\partial x}\frac{\partial^2 w}{\partial y^2} + 2A_{66}\cdot\frac{\partial u}{\partial y}\frac{\partial^2 w}{\partial x \partial y};$$

$$P_6(v,w) = A_{11}\frac{\partial v}{\partial y}\frac{\partial^2 w}{\partial y^2} + \nu\cdot A_{11}\frac{\partial v}{\partial y}\frac{\partial^2 w}{\partial x^2} + 2A_{66}\cdot\frac{\partial v}{\partial x}\frac{\partial^2 w}{\partial x \partial y}$$

Equations (11) can be used to investigate nonlinear vibration and dynamic stability of variable thickness FGM circular cylinder shell under mechanical load.

3 Solution Method

The present article considers a variable thickness FGM cylindrical shell with simply supported at both ends, under uniform external pressure *q(t)* and axial compression force *p(t).*

The boundary conditions are:

$w=0$, $N_{xy}=0$, $M_{xx}=0$, $N_{xx}=-p.h$ at $x=0$ and $x=L$

Displacement components of the cylindrical shell can be expanded as:

$$\begin{cases} u = U_{mn}(t)\cos\alpha x\,\sin\beta y; \\ v = V_{mn}(t)\sin\alpha x\,\cos\beta y; \\ w = W_{mn}(t)\sin\alpha x\,\sin\beta y. \end{cases} \tag{12}$$

in which $\alpha = \frac{m\pi}{L}$; $\beta = \frac{n}{R}$. *m, n*—the half-waves number in x and y direction, respectively.

Substituting Eq. (12) in Eq. (11), then applying Galerkin procedure yields:

$$\begin{cases} I_{11}U + I_{12}V + I_{13}W + R_1W^2 = \rho_1^{**}\dfrac{d^2U}{dt^2} \\ I_{21}U + I_{22}V + I_{23}W + R_2W^2 = \rho_1^{**}\dfrac{d^2V}{dt^2} \\ I_{31}U + I_{32}V + I_{33}W + R_3W^2 + R_4W^3 + R_5U\cdot W + R_6V\cdot W + \dfrac{pm^2\pi^3(La+2b)R}{8L}\cdot W \\ +\dfrac{4\delta_n\delta_m RLq}{mn\pi} = \rho_1^{**}\dfrac{d^2W}{dt^2} + 2\varepsilon\rho_1^{**}\dfrac{dW}{dt} \end{cases} \tag{13}$$

in which

$$\rho_1^{**} = \frac{\rho_1^* L(La+2b)\pi R}{8};\ \delta_n = \frac{(-1)^n-1}{2};\ \delta_m = \frac{(-1)^m-1}{2};$$

$$I_{11} = \frac{E_1\pi\left((\nu-1)n^2L^2 - 2\pi^2R^2m^2\right)(La+2b)}{16RL(1-\nu^2)};$$

$$I_{12} = I_{21} = \frac{E_1 m\pi^2 n(La+2b)}{16(1-\nu^2)};$$

$$I_{13} = \frac{E_1\nu m\pi^2(La+2b)}{8(1-\nu^2)} - \frac{E_2\Delta(\pi^2R^2m^2+L^2n^2\nu)}{24L^2Rm(1-\nu^2)} + \frac{E_2n^2\Delta}{24(1+\nu)mR};$$

$$R_1 = \frac{2E_1\left(2\pi^2R^2m^2 - L^2n^2\nu\right)(La+2b)}{9L^2Rn\left(\nu^2-1\right)} - \frac{E_1n(La+2b)}{9(1+\nu)R};\ I_{22} = \frac{E_1\pi(La+2b)\left(2L^2n^2 - R^2m^2(\nu-1)\pi^2\right)}{16(\nu^2-1)LR};$$

$$I_{23} = -\frac{E_1\pi Ln(La+2b)}{8R\left(1-\nu^2\right)} + \frac{E_2n\left(3L^4a^2n^2 - n^2\left(R^2m^2\pi^2+L^2\right)\left(\Delta-3L^2a^2\right) + 3(2\nu-1)m^2\pi^2L^2R^2a^2\right)}{24(\nu^2-1)R^2Lm^2\pi};$$

$$R_2 = \frac{2E_1\left(2L^2n^2 - \pi^2R^2m^2\nu\right)(La+2b)}{9R^2Lm\pi(\nu^2-1)} - \frac{E_1m\pi(La+2b)}{9(1+\nu))L};$$

$$I_{31} = -\frac{\nu E_1m\pi^2(La+2b)}{8\left(1-\nu^2\right)} - \frac{E_2\left(m^2\pi^2R^2+L^2n^2\nu\right)\left(\Delta-3L^2a^2\right) - 3L^2a^2}{24L^2Rm\left(\nu^2-1\right)} + \frac{E_2n^2\Delta}{24m(1+\nu)R};$$

$$I_{32} = \frac{E_1Ln\pi(La+2b)}{8R\left(\nu^2-1\right)} - \frac{E_2L\left(\Delta-6L^2a^2\right)n^3}{24m^2\pi R^2(\nu^2-1)} + \frac{E_2n\Delta\pi}{24(1+\nu)L};$$

$$I_{33} = \frac{E_1 L(La+2b)\pi}{8R(\nu^2-1)} + \frac{E_2\left[3L^4a^2n^2 - \left(\nu R^2m^2\pi^2 + 2n^2L^2\right)\left(\Delta - 3L^2a^2\right) - 6m^2\pi^2(2R-3)\nu R^2L^2a^2\right]}{12R^2L\pi m^2(\nu^2-1)}$$
$$+ \frac{E_3(La+2b)\left(m^4\pi^4R^2\left[\left(R^2m^2\pi^2 + 2n^2L^2\nu\right)\Delta^* - 3L^2R^2a^2\right] + L^4n^4\left[m^2\pi^2\left(\Delta^* + 6\nu R^2a^2\right) - 3L^2a^2\right]\right)}{16\pi m^2(\nu^2-1)R^3L^3}$$
$$- \frac{E_3\pi(m^2\Delta^*\pi^2 + 3L^2a^2)(La+2b)}{8(1+\nu)LR};$$

$$R_3 = -\frac{2E_1\left(5L^2n^2 - 3\pi^2R^2m^2\nu\right)(La+2b)}{9LR^2mn\pi(\nu^2-1)} + \frac{8a^2E_2\left(L^2n^2\nu - 11R^2m^2\pi^2\right)}{27LRmn\pi(\nu^2-1)}$$
$$\frac{4E_2\left[9\left(R^4m^4\pi^4 + L^4n^4\right)m^2\pi^2\Delta^* - 4L^2a^2\left(7R^4m^4\pi^4 - 10L^4n^4\right)\right]}{81L^3R^3m^3\pi^3n(\nu^2-1)} + \frac{4E_2n\nu(\left(9m^2\pi^2\Delta^* - 44L^2a^2\right)}{27LRm\pi(\nu^2-1)}$$
$$+ \frac{8E_2n\nu\left(9m^2\Delta^*\pi^2 - 34L^2a^2\right)}{81LRm\pi(\nu^2-1)} + \frac{16E_2a^2Ln}{27Rm\pi(1+\nu)} + \frac{2E_2n(\left(4L^2a^2 - 9m^2\pi^2\Delta^*\right)}{81LRm\pi(1+\nu)}$$

$$R_4 = \frac{3E_1\pi\left(\pi^4R^4m^4 + 2L^2\pi^2R^2m^2n^2\nu + L^4n^4\right)(La+2b)}{256R^3L^3(\nu^2-1)} + \frac{E_1m^2\pi^3n^2(La+2b)}{128L(1+\nu)R}$$

$$R_5 = -\frac{8E_1\left(\pi^2R^2m^2 + L^2n^2\nu\right)(La+2b)}{9L^2Rn(\nu^2-1)} + \frac{2E_1n(La+2b)}{9(1+\nu)R};$$

$$R_6 = \frac{8E_1\left(\nu R^2m^2\pi^2 + L^2n^2\right)(La+2b)}{9R^2Lm\pi\left(1-\nu^2\right)} + \frac{2E_1m\pi(La+2b)}{9L(1+\nu)};$$

$$\Delta = 2\pi^2m^2\left(L^2a^2 + 3Lab + 3b^2\right) + 3L^2a^2;\ \Delta^* = \left(L^2a^2 + 2Lab + 2b^2\right)$$

According to Volmir's assumption (Volmir 1972), by ignoring the inertial components along x and y axes (u< <w, v< <w), Eqs. (13) can be rewritten as:

$$\begin{cases} I_{11}U + I_{12}V + I_{13}W + R_1W^2 = 0 \\ I_{21}U + I_{22}V + I_{23}W + R_2W^2 = 0 \\ I_{31}U + I_{32}V + I_{33}W + R_3W^2 + R_4W^3 + R_5U\cdot W + R_6V\cdot W + \dfrac{pm^2\pi^3(La+2b)R}{8L}\cdot W \\ + \dfrac{4\delta_n\delta_m RL}{mn\pi}q = \rho_1^{**}\dfrac{d^2W}{dt^2} + 2\varepsilon\rho_1^{**}\dfrac{dW}{dt} \end{cases} \tag{14}$$

Table 1 Natural frequencies of FGM cylindrical shell (Hz)

n	h/R = 0.002, L/R = 20; k = 2, m = 1		
	Present (17)	Loy et al. (1999)	Bich et al. 2012
1	13.1266	13.321	13.3211
2	4.5830	4.5114	4.5173
3	4.5110	4.1827	4.1911
4	7.4257	7.0905	7.0959
5	11.6061	11.329	11.3329
6	16.7835	16.587	16.5896
7	22.9174	22.454	22.8201
8	29.9995	30.014	30.0148
9	38.0276	38.171	38.1711
10	47.0008	47.288	47.2881

Table 2 The comparison vibration frequency of constant thickness FGM shell (1/s)

k	R/h = 500, L/R = 2; m = 1			
	$n = 1$		n = 3	
	Present (18)	Bich et al. (2012)	Present (18)	Bich et al. 2012
0	3702.65	3702.65	1120.02	1120.05
1	3605.32	3605.41	1090.01	1090.63
3	3566.52	3566.62	1078.25	1078.25
5	3523.72	3523.79	1065.47	1065.47
∞	3476.27	3476.27	1051.57	1051.57

Table 3 Critical stress of FGM cylindrical shell (Mpa)

Source	R/h = 500; L/R = 2;			
	$k=0.2$	$k=0.5$	$k=1.0$	$k=5.0$
Huang et al. (2010)	194.94 (2, 11)	182.49 (2, 11)	169.94 (2, 11)	150.25 (2, 11)
Present	199.30 (1, 13)	185.37 (1, 13)	175.63 (1, 13)	160.16 (1, 13)

Table 4 Natural frequencies of variable thickness FGM cylindrical shell (1/s)

k	$h_1=0.004$ m, $h_0=0.006$ m, $R/h=200$, $L/R=2$				
	(m, n) = (1, 1)	(m, n) = (1, 3)	(m, n) = (1, 5)	(m, n) = (1, 7)	(m, n) = (1, 9)
0	5930.10	1796.32	797.43	662.16	900.89
0.5	5322.10	1607.68	700.68	559.95	756.35
1	4932.38	1487.72	641.99	502.50	676.96
3	4173.35	1257.02	540.56	429.56	589.71
5	3849.00	1160.12	502.99	413.90	577.28
∞	3019.55	914.66	405.88	337.03	458.54

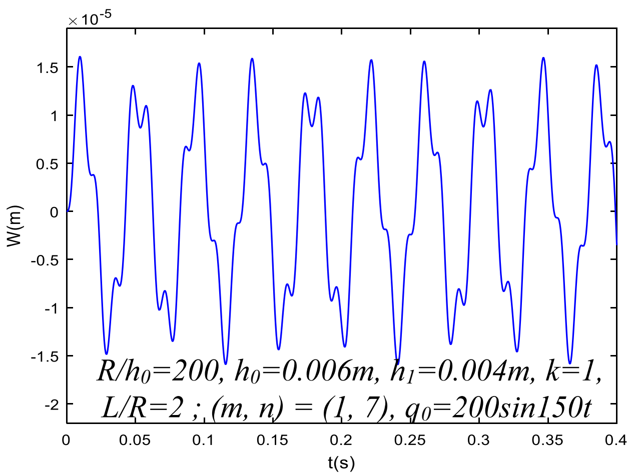

Fig. 2 Nonlinear dynamic response of variable thickness FGM cylindrical shell

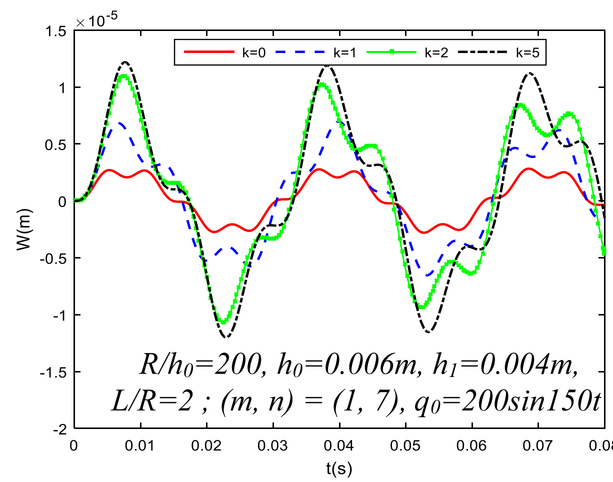

Fig. 4 Effect of volume fraction (k) on the dynamic response of variable thickness cylindrical shell

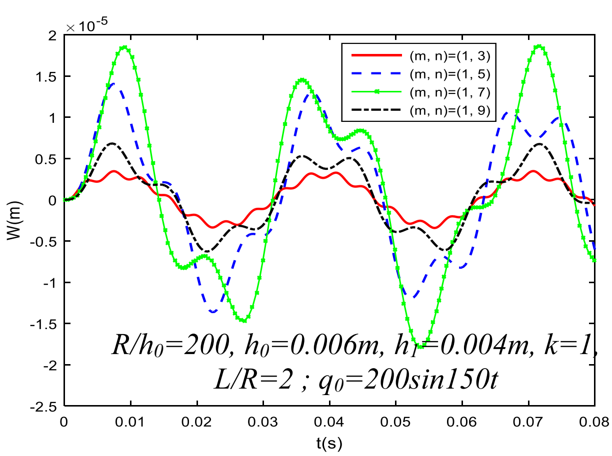

Fig. 3 Effect of vibration mode on response amplitude of the shell

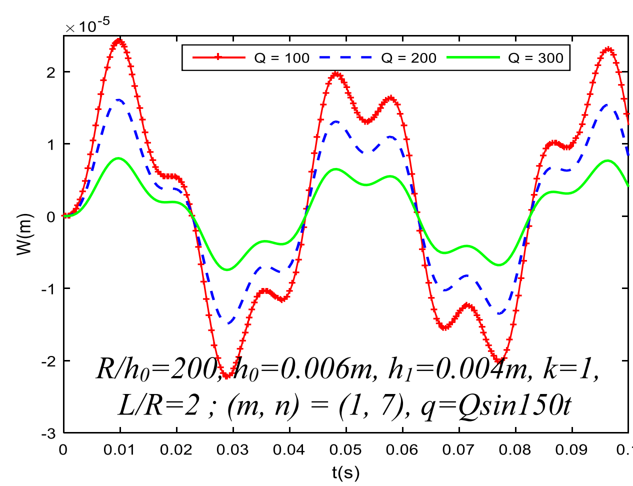

Fig. 5 Effect of excitation force on nonlinear dynamic response of variable thickness cylindrical shell

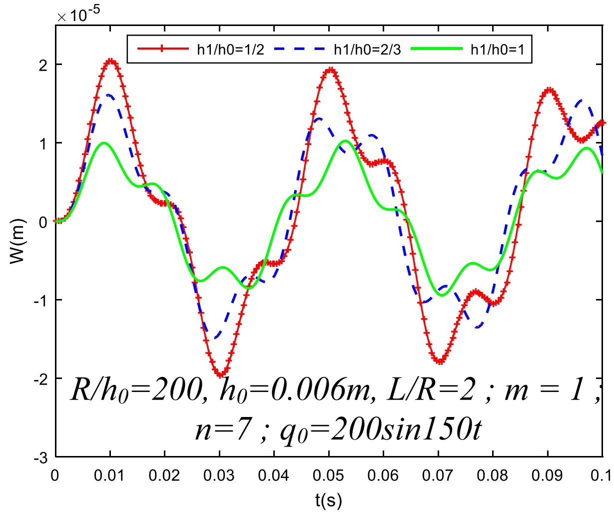

Fig. 6 Influence of h_1/h_0 ratio on nonlinear dynamic responses of variable thickness cylindrical shell

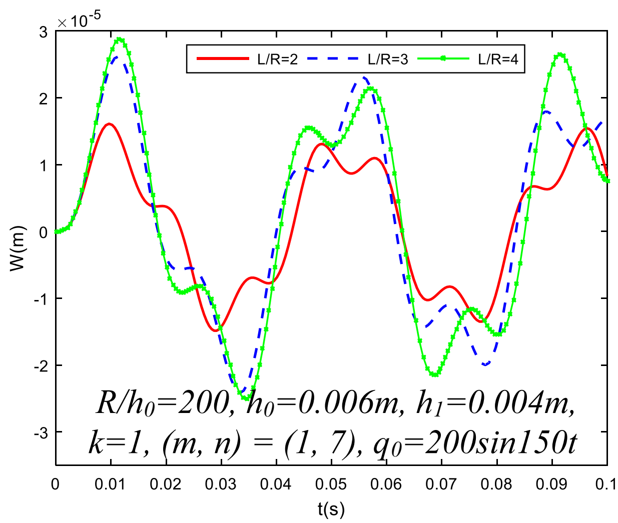

Fig. 7 Influence of L/R ratio on nonlinear dynamic response of variable thickness cylindrical shell

From the first two equations of Eq. (14), we obtain U_{mn} and V_{mn} in terms of W_{mn} then substituting in the third equation, we have

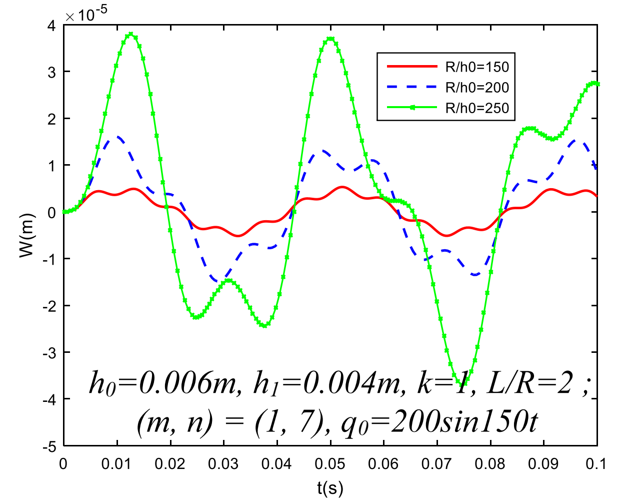

Fig. 8 Influence of R/h_0 ratio on the nonlinear dynamic responses of variable thickness cylindrical shell

$$a_3 = -R_4 - \frac{R_5\left(R_2 I_{12} - R_1 I_{22}\right) + R_6\left(R_1 I_{21} - R_2 I_{11}\right)}{I_{11} I_{22} - I_{12} I_{21}}$$

Assume that uniformly distributed pressure in the form $q(t) = Q\sin\Omega t$, Eq. (15) can be rewritten as:

$$\begin{vmatrix} I_{11} + \rho_1^{**}\omega^2 & I_{12} & I_{13} \\ I_{12} & I_{22} + \rho_1^{**}\omega^2 & I_{23} \\ I_{31} & I_{32} & I_{33} + \rho_1^{**}\omega^2 \end{vmatrix} = 0 \tag{16}$$

3.1 Nonlinear Dynamic Response Analysis

3.1.1 NATURAL Frequencies

Natural frequencies of variable thickness FGM shell can be determined from Eq. (13) by solving the equation:

$$\rho_1^{**}\frac{d^2W}{dt^2} + 2\varepsilon\rho_1^{**}\frac{dW}{dt} + a_1 W + a_2 W^2 + a_3 W^3 - \frac{pm^2\pi^3(La + 2b)R}{8L}\cdot W - \frac{4\delta_n\delta_m RL}{mn\pi}q = 0 \tag{15}$$

in which

$$a_1 = -I_{33} - \frac{I_{31}\left(I_{12}I_{23} - I_{13}I_{22}\right) + I_{32}\left(I_{13}I_{21} - I_{11}I_{23}\right)}{I_{11}I_{22} - I_{12}I_{21}}$$

$$\begin{vmatrix} I_{11} + \rho_1^{**}\omega^2 & I_{12} & I_{13} \\ I_{12} & I_{22} + \rho_1^{**}\omega^2 & I_{23} \\ I_{31} & I_{32} & I_{33} + \rho_1^{**}\omega^2 \end{vmatrix} = 0 \tag{17}$$

$$a_2 = -R_3 - \frac{R_1\left(I_{32}I_{21} - I_{31}I_{22}\right) + R_2\left(I_{31}I_{12} - I_{32}I_{11}\right) + R_5\left(I_{12}I_{23} - I_{13}I_{22}\right) + R_6\left(I_{13}I_{21} - I_{11}I_{23}\right)}{I_{11}I_{22} - I_{12}I_{21}}$$

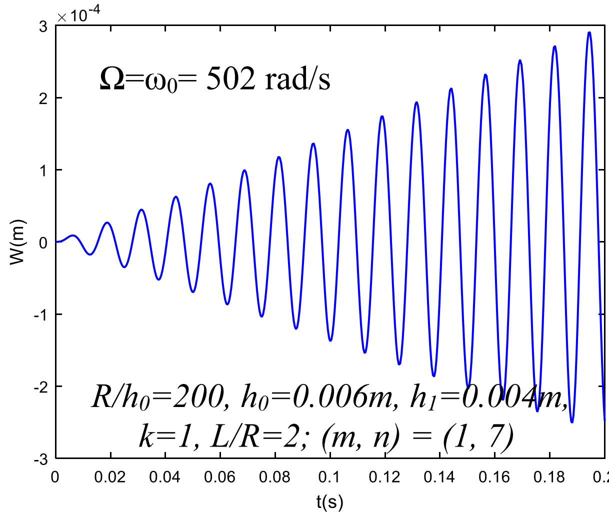

Fig. 9 Resonance phenomenon

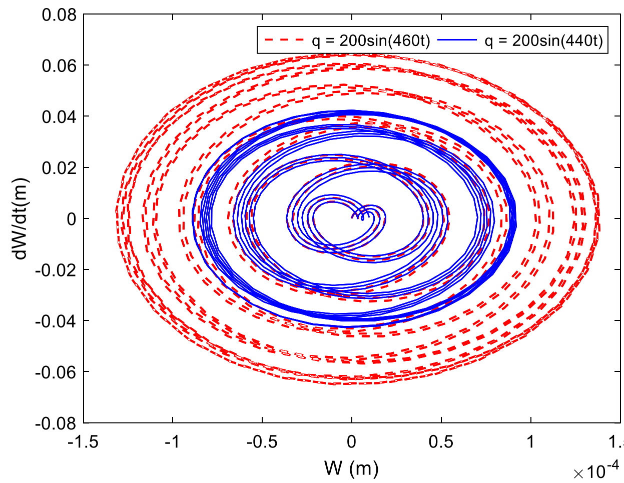

Fig. 11 The dw/dt-w relationships

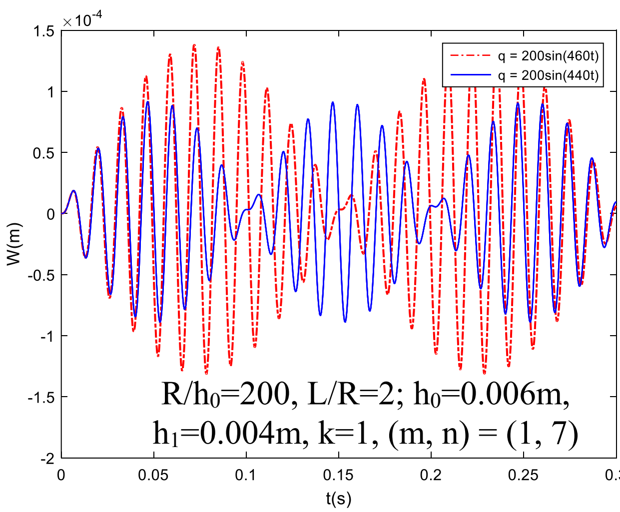

Fig. 10 The harmonic beat phenomenon

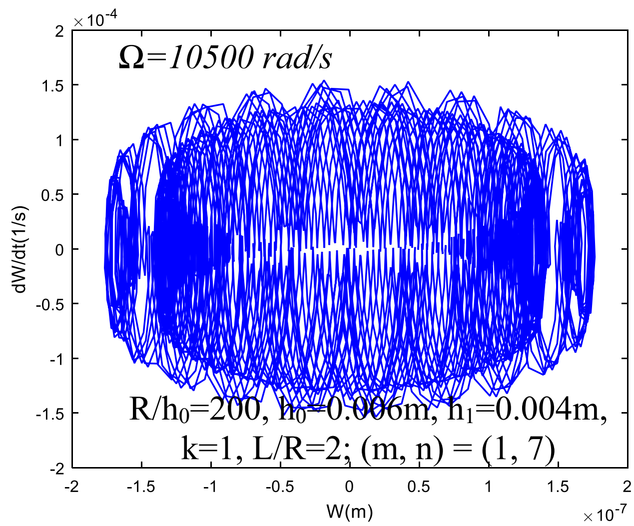

Fig. 12 The dw/dt -w relationship curves in cases of $\Omega >> \omega_0$

3.1.2 Nonlinear Dynamic Responses of the Variable Thickness Cylindrical Shell

Nonlinear dynamic responses of variable thickness cylindrical shells can be obtained from Eq. (16) by using Runge–Kutta method and shown in the numerical results.

In other hand, natural frequencies of the structure can be obtained from Eq. (16) and expressed as:

$$\omega_0 = \sqrt{\frac{a_1 - \frac{pm^2\pi^3(La+2b)R}{8L}}{\rho_1^{**}}} = \sqrt{-\frac{I_{33}}{\rho_1^{**}} - \frac{I_{31}\left(I_{12}I_{23}-I_{13}I_{22}\right) + I_{32}\left(I_{13}I_{21}-I_{11}I_{23}\right)}{\rho_1^{**}\left(I_{11}I_{22}-I_{12}I_{21}\right)} - \frac{pm^2\pi^3(La+2b)R}{8L\rho_1^{**}}} \tag{18}$$

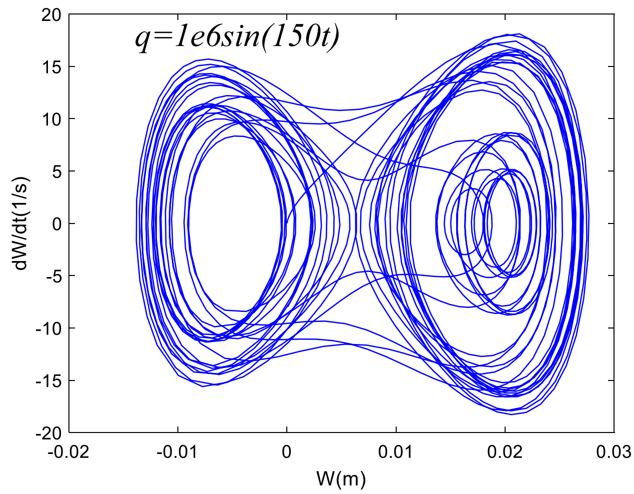

Fig. 13 The dw/dt -w relationship curves in case of very great excitation force intensity

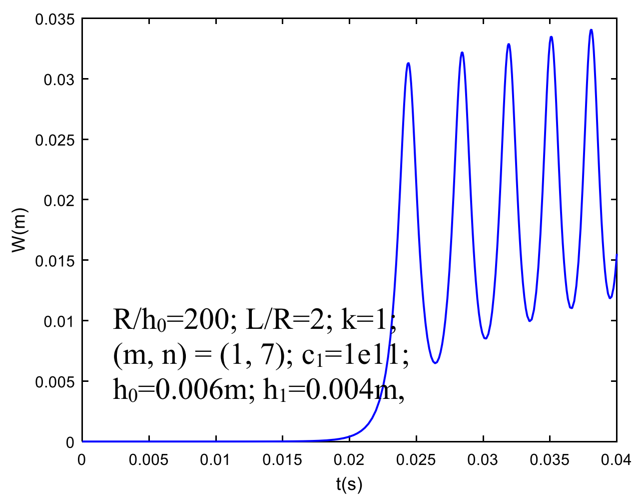

Fig. 14 Nonlinear dynamic responses of variable thickness FGM shell

3.2 Dynamic Stability Analysis

Analyze nonlinear dynamic stability of variable thickness FGM shell in two cases as follows:

Case 1 Variable thickness FGM cylindrical shell subjected to axial compression load in terms of time $p=-c_1t$ (c_1-loading speed); $q=0$.

Case 2 Variable thickness FGM shell under axial compression load $p=constant$ and uniformly distributed pressure in terms of time $q=c_2t$ (c_2- loading speed).

Solving Eq. (16) for each case, we obtain dynamic responses of the shell. Dynamic critical time t_{cr} is obtained according to Budiansky–Roth criterion (Volmir, 1962), and dynamic critical loads can be determined as follows: $p_{cr}=c_1t_{cr}$ (case 1), $q_{cr}=c_2t_{cr}$ (case 2).

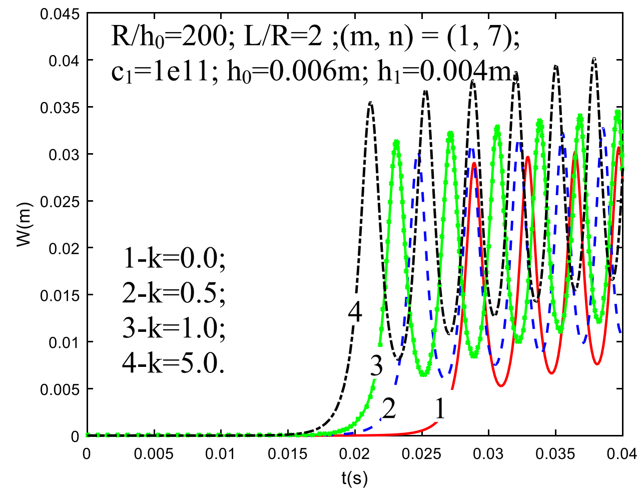

Fig. 15 Nonlinear dynamic responses of the shell with various values of k

Table 5 The critical load of FGM shell with various values of k (GPa)

R/h_0	$L/R=2;\ (m,\ n)=(1,\ 7);\ c_1=1e11;\ h_0=0.006\ m;\ h_1=0.004\ m$			
	k = 0	k = 0.5	k = 1	k = 5
200	2.846	2.423	2.256	2.062
300	3.057	2.825	2.723	2.563
400	3.493	3.309	3.198	3.061

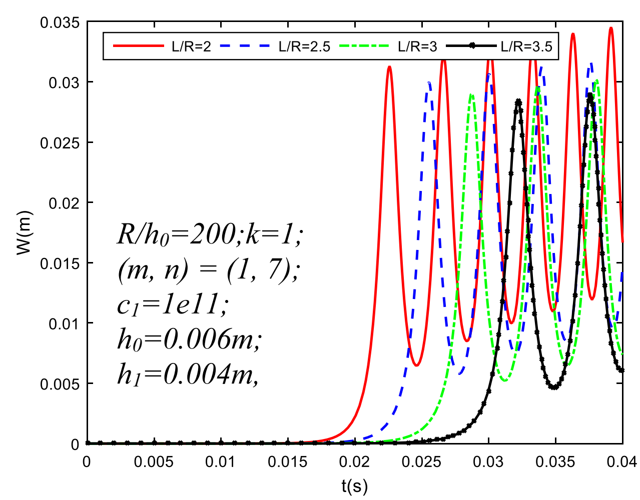

Fig. 16 Effect of L/R ratio on dynamic responses of variable thickness FGM shell

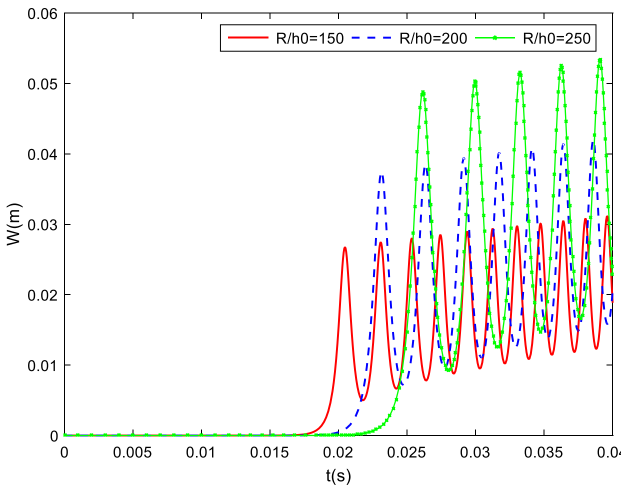

Fig. 17 Effect of R/h_0 ratio on dynamic responses of variable thickness FGM shell

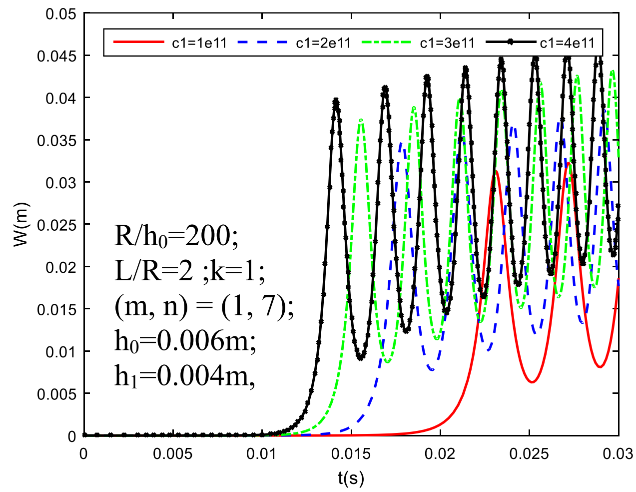

Fig. 19 Influence of loading speed on the dynamic response of the FGM shell

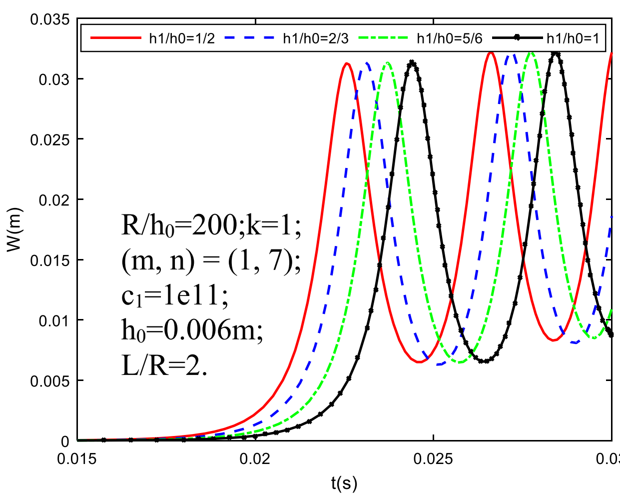

Fig. 18 Effects of h_1/h_0 ratio on dynamic response of the FGM shell

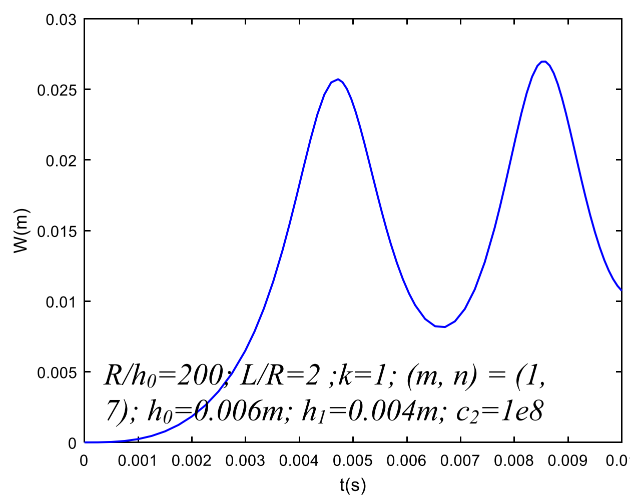

Fig. 20 Dynamic response of variable thickness FGM shell

4 Validation

To verify the reliability of the proposed method, the obtained results of the present article are compared with results in the published work of Bich et al. (2012) and Loy et al. (1999). They studied on the vibration of FGM cylindrical shell made of stainless steel and nickel with material properties $\nu_c = \nu_m = 0.31$; $E_m = 207{,}788.10^9$ N/m^2, $\rho_m = 8166$ kg/m^3 and $E_c = 205{,}098.10^9$ N/m^2, $\rho_c = 8900$ kg/m^3. Comparison results are shown in Table 1.

Besides that, natural frequencies (1/s) obtained in present paper are also compared with those in publication of Bich et al. (2012) for FGM cylinder shell made of ZrO_2/Ti–6Al–4 V, material properties are: $\nu_c = \nu_m = 0.2981$; $E_m = 105{,}696.10^9$ N/m^2, $\rho_m = 4429$ kg/m^3, $E_c = 154.10^9$ N/m^2, $\rho_c = 5700$ kg/m^3. The comparison results are shown in Table 2.

Moreover, the critical stress of the structures in present study was compared with results in publication of Huang et al. (2010) for FGM cylindrical shell made of ZrO_2/Ti-6Al-4 V with material properties are: $E_m = 122.56$ GPa; $\rho_m = 4429$ kg/m^3; $\nu_m = 0.288$; $E_c = 244.27$ GPa; $\rho_c = 5700$ kg/m^3; $\nu_c = 0.288$. Comparison results are shown in Table 3

The comparisons show that results in the present paper are good agreement with those in the above literature. Therefore, the proposed method is completely accurate and reliable for solving the forced vibration and dynamic

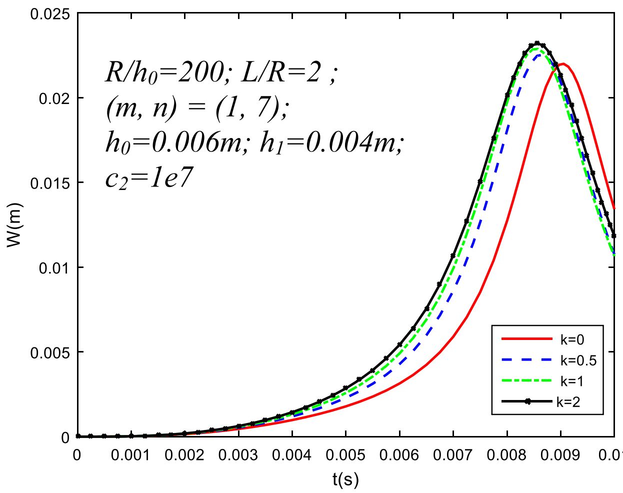

Fig. 21 Dynamic response of variable thickness FGM shell with various k

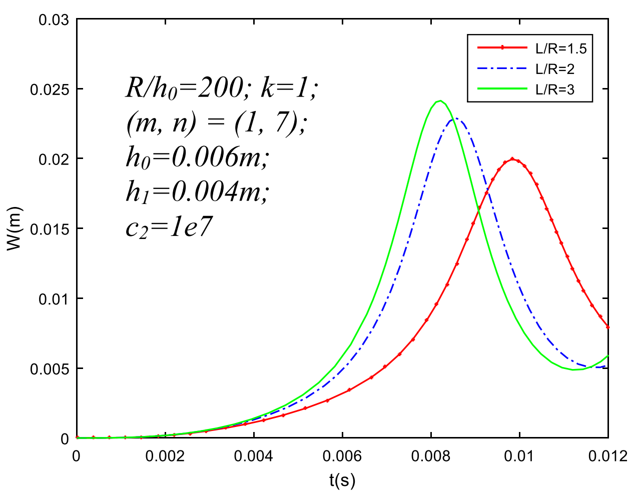

Fig. 22 Effect of L/R ratio on the dynamic response of the shell

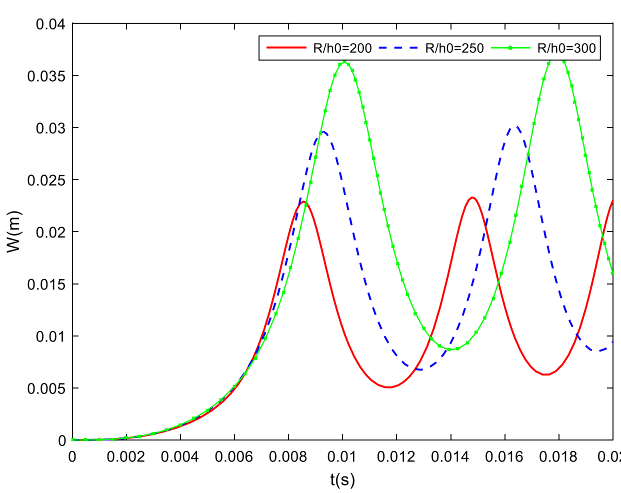

Fig. 23 Effect of R/h_0 ratio on dynamic response of the shell

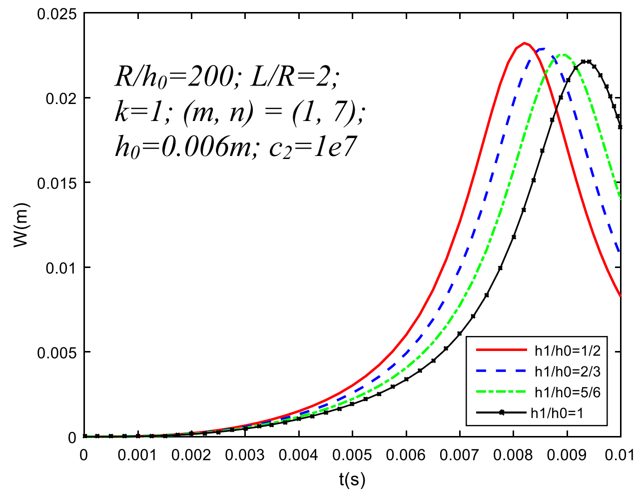

Fig. 24 Effects of h_1/h_0 ratio on the dynamic response of variable thickness FGM shell

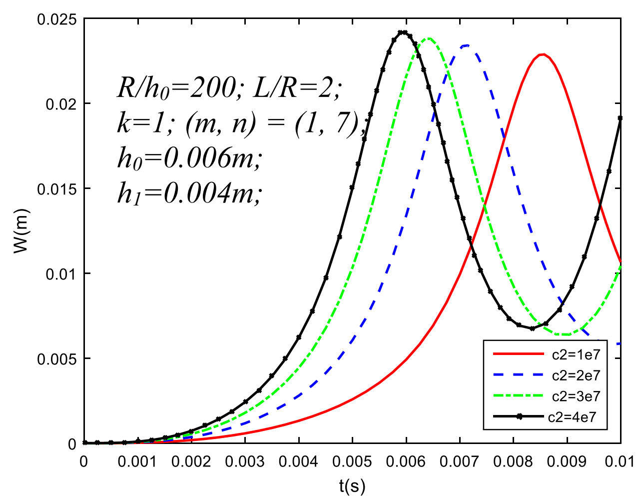

Fig. 25 Dynamic response of the FGM shell with the various loading speed

buckling problems of the FGM cylindrical shell with variable thickness.

5 Numerical Results

Consider a variable thickness FGM cylindrical shell made of aluminum and alumina with geometric dimensions: $h_1 = 0.006$ m, $h_0 = 0.004$ m, $R/h_0 = 200$, $L/R = 2$. Material properties: $E_m = 70.10^9$ N/m^2, $\rho_m = 2702$ kg/m^3 and $E_c = 380.10^9$ N/m^2, $\rho_c = 3800$ kg/m^3, $\nu_m = \nu_c = 0.3$. Assume that the shell is simply supported at both ends.

5.1 Nonlinear Vibration Analysis

5.1.1 Natural Vibration Frequencies

Natural frequencies of the shell are determined according to Eq. (18) and shown in Table 4. We can see that natural frequencies of structure depend on volume fraction (k) and vibration mode (m, n). In the present paper, the lowest natural frequency corresponding to vibration mode (m, n) = (1, 7).

5.1.2 Nonlinear Dynamic Responses of Variable Thickness FGM Cylindrical Shell

Nonlinear dynamic responses of variable thickness FGM cylindrical shell can be obtained from Eq. (16) by using the fourth-order Runge–Kutta method. Figure 2 demonstrates the nonlinear dynamic responses of variable thickness FGM cylinder shell, simply supported at both ends and subjected to mechanical load. The effects of vibration mode on natural frequencies and nonlinear dynamic responses of variable thickness shell are shown in Table 4 and Fig. 3. We can see that, corresponding to the nonlinear vibration mode (m, n) = (1, 7), the nonlinear vibration amplitude of the shell is the greatest.

Nonlinear dynamic responses of variable thickness FGM shell with the various values of k are demonstrated in Fig. 4. The graph shows that vibration amplitude of the structure increases when value of k index increases. The cause of this phenomenon is that the value of k increases, the metal ratio in the structure increases, and therefore, the stiffness of the structure decreases and the amplitude of nonlinear dynamic response of the shell increases. The influences of excitation force intensity on the nonlinear dynamic response of the shell are shown in Fig. 5.

Influences of geometric dimensions on nonlinear dynamic responses of variable thickness FGM cylindrical shell are shown in Figs. 6, 7 and 8. The graphs show that the larger the L / R ratio (or R / h_0 ratio) is, the greater the vibration amplitude of the shell get. In other words, the greater the length (or radius) of the structure is, the lower the stiffness of the structure is.

Nonlinear vibration characteristics of FGM cylindrical shell with variable thickness are investigated and presented in Figs. 9, 10, 11, 12 and 13.

Resonance phenomenon will occur when the frequency of the excitation force is equal to the natural frequency of the shell $\Omega = \omega_{0(1,7)} = 502$ (rad/s). Then nonlinear vibration amplitude of the shell will infinitely increase over time (Fig. 9).

When excitation frequency is close to the natural frequencies of the shell, the harmonic beat phenomenon will occur and shown in Fig. 10. The closer the excitation frequency is, the greater the dynamic responses amplitude and the vibration period are. The velocity–deflection relationships are closed curves shown in Fig. 11.

When frequencies of excitation force are far from natural frequencies of the shell ($\Omega >> \omega_0$), the deflection–velocity relationship becomes very complex curves (Fig. 12).

When increasing the intensity of excitation force to very great value, the velocity-deflection relationship becomes disturbed curves (Fig. 13).

5.2 Nonlinear Dynamics Stability of Variable Thickness FGM Shell

Case 1 Variable thickness FGM cylindrical shell subjected to axial compression load in terms of time $p = -c_1 t$ (c_1-loading speed); $q = 0$ (Fig. 14).

The effects of volume fraction (index k) on nonlinear dynamic responses of variable thickness FGM shell are demonstrated in Fig. 15 and Table 5. We can see that when values of k increase, the critical load of structure decreases. This is reasonable because the higher the value of k is, the greater the metal volume fraction is, which lead to the stiffness of structure decrease and the stability capable of the shell decrease.

The effects of geometric parameters on the nonlinear dynamic response of the variable thickness FGM cylindrical shell are shown in Figs. 16, 17, and 18. It can be seen that the critical load of the structure increases when L/R (or R/h_0) ratio increases (Fig. 16 and 17), which means the stability capacity of the shell will increase when the length (or radius) of structure increases.

The effect of h_1/h_0 ratio on the nonlinear dynamic response of the cylindrical shell is shown in Fig. 18. We can see that, with the increasing h_1/h_0 ratio, the dynamic critical load of structure also increases. The dynamic critical load of the shell reaches its maximum value when $h_1/h_0 = 1$.

Influences of loading speed on nonlinear dynamic response of the shell are shown in Fig. 19. The graph shows that the greater the loading speed is, the lower the critical time is and the greater the dynamic critical load is. That means, with the higher loading speed, the stability loss of the shell will occur faster and at the greater critical load.

Case 2 Variable thickness FGM cylindrical shell under axial compression load $p = constant$ and uniformly distributed pressure in terms of time $q = c_2 t$ (c_2- loading speed).

The nonlinear dynamic responses of variable thickness FGM cylindrical shell, in this case, are demonstrated in Fig. 20, 21, 22, 23, 24 and 25.

Effects of volume fraction index (k) on the dynamic response of variable thickness cylinder shell are shown in Fig. 21. We can see that the critical load will decrease with the increase in volume fraction index (k). In other words, the stability capacity of structure will decrease.

When L/R ratio increases, the dynamic critical loads of the shell decrease (Fig. 22). It means the greater the length of the structure is, the less the pressure-bearing capacity of the shell is.

Figure 23 shows the effect of R/h_0 ratio on nonlinear dynamic responses of the shell. It can be seen that if the value of R/h_0 ratio increases, dynamic critical pressure will increase. That means the bearing capacity of bigger shell will better than small one.

The effects of h_1/h_0 ratio on the nonlinear dynamic response of the shell are similar to those in case 1, and the critical load of cylindrical shell reaches a maximum value when $h_1/h_0 = 1$ (constant thickness FGM shell) (Fig. 24).

The effects of loading speed on the nonlinear dynamic response of the shell are shown in Fig. 25. The graph shows that the greater the loading speed is, the lower the critical time and the greater the critical pressure are. In other words, with the higher loading speed, the stability loss will occur faster and at the greater critical pressure.

6 Conclusions

By using an analytical approach, based on the thin shell theory, taking into account the nonlinear geometry of von Karman–Donnell, nonlinear vibration and stability problems of variable thickness FGM cylindrical shell are solved by using Galerkin method and the fourth-order Runge–Kutta method.

Some following conclusions can be drawn from the examined results:

- Natural frequencies of variable thickness FGM shell depending on volume fraction index (k) and the vibration mode (m, n).
- Geometric parameters of the shell (L, R, h_1, h_0) are factors effect on the nonlinear vibration amplitude of the structure. When geometric dimensions of the shell increase (L, R), dynamic responses amplitude of the shell will increase, which means the stiffness of structure decreases.
- When the excitation frequency is greater than the natural frequency of the shell, the deflection–velocity relationships are closed curves. If the frequency and intensity of excitation force is very great, the deflection–velocity curves become very complex and disturbed curves
- Volume fraction index (k) remarkably affects the dynamic critical load of the structure. The greater the volume fraction index is, the lower the critical load of the shell is. In other words, the metal-richer FGM shell will work less stability than ceramic-richer ones.
- When the length (L) of cylindrical shell increases, the dynamic critical load in case of axial compression-bearing shell increases, but the critical load in case of external pressure-bearing shell decreases. That means, if the length of structure increase, the axial compression-bearing capacity of the shell increases but the external pressure-bearing capacity of the shell decreases.
- If the value of loading speed increases, the stability loss of the shell will occur faster and at greater dynamic critical load.

Funding This research is funded by Vietnam National Foundation for Science and Technology Development (NAFOSTED) under grant number 107.02–2018.324.

References

Aksogan O, Sofiyev AH (2002) Dynamic buckling of a cylindrical shell with variable thickness subject to a time dependent external pressure. J Sound Vib 254(4):693–702. https://doi.org/10.1006/jsvi.2001.4115

Alibeigloo A, Noee ARP (2017) Static and free vibration analysis of sandwich cylindrical shell based on theory of elasticity and using DQM. Acta Mech 228(12):4123–4140. https://doi.org/10.1007/s00707-017-1914-4

Avramov KV (2011) Nonlinear modes of vibrations for simply supported cylindrical shell with geometrical nonlinearity. Acta Mech 223(2):279–292. https://doi.org/10.1007/s00707-011-0556-1

Bacciocchi M, Eisenberger M, Fantuzzi N, Tornabene F, Viola E (2016) Vibration analysis of variable thickness plates and shells by the generalized differential quadrature method. Compos Struct 156:218–237. https://doi.org/10.1016/j.compstruct.2015.12.004

Bich DH, Nguyen NX (2012) Nonlinear vibration of functionally grade circular cylindrical shells based on improved Donnell equations. J Sound Vib 331(25):5488–5501. https://doi.org/10.1016/j.jsv.2012.07.024

Brush DO, Almroth BO (1975) Buckling of bars, plates and shells. Mc Graw-Hill Inc

Budiansky B, Roth RS (1962) Axisymmetric dynamic buckling of clamped shallow spherical shells. NASA Technical Note D.510, 597–609

Dat ND, Khoa ND, Nguyen PD, Duc ND (2019) An analytical solution for nonlinear dynamic response and vibration of FG-CNT reinforced nanocomposite elliptical cylindrical shells resting on elastic foundations. ZAMM J Appl Math. https://doi.org/10.1002/zamm.201800238

Deniz A, Sofiyev AH (2013) The nonlinear dynamic buckling response of functionally graded truncated conical shells. J Sound Vib 332:978–992. https://doi.org/10.1016/j.jsv.2012.09.032

Duc ND (2013) Nonlinear dynamic response of imperfect eccentrically stiffened FGM double curved shallow shells on elastic foundation. J Compos Struct 102:306–314. https://doi.org/10.1016/j.compstruct.2012.11.017

Duc ND (2014) Nonlinear Static and Dynamic Stability of Functionally Graded Plates and Shells. Vietnam National University Press, Hanoi

Duc ND (2016) Nonlinear thermal dynamic analysis of eccentrically stiffened S-FGM circular cylindrical shells surrounded on elastic foundations using the Reddy's third-order shear deformation shell theory. J Eur J Mech A/Solids 58:10–30. https://doi.org/10.1016/j.euromechsol.2016.01.004

Duc ND, Quan TQ (2014) Nonlinear response of imperfect eccentrically stiffened FGM cylindrical panels on elastic foundation subjected to mechanical loads. Eur J Mech A Solids 46:60–71. https://doi.org/10.1016/j.euromechsol.2014.02.005

Duc ND, Thang PT (2014a) Nonlinear response of imperfect eccentrically stiffened ceramic-metal-ceramic FGM thin circular cylindrical shells surrounded on elastic foundations and subjected to axial compression. Compos Struct 110:200–206. https://doi.org/10.1016/j.compstruct.2013.11.015

Duc ND, Thang PT (2014b) Nonlinear buckling of imperfect eccentrically stiffened metal-ceramic-metal S-FGM thin circular cylindrical shells with temperature-dependent properties in thermal environments. Int J Mech Sci 81:17–25. https://doi.org/10.1016/j.ijmecsci.2014.01.016

Duc ND, Thang PT (2015) Nonlinear response of imperfect eccentrically stiffened ceramic-metal-ceramic S-FGM thin circular cylindrical shells surrounded on elastic foundations under uniform radial load. J Mech Adv Mater Struct 22:1031–1038. https://doi.org/10.1080/15376494.2014.910320

Duc ND, Thang PT, Dao NT, Tac HV (2015) Nonlinear buckling of higher deformable S-FGM thick circular cylindrical shells with metal-ceramic-metal layers surrounded on elastic foundations in thermal environment. J Compos Struct 121:134–141. https://doi.org/10.1016/j.compstruct.2014.11.009

Dung DV, Hoa LK (2015) Nonlinear torsional buckling and postbuckling of eccentrically stiffened FGM cylindrical shells in thermal environment. Compos Part B 69:378–388. https://doi.org/10.1016/j.compositesb.2014.10.018

Dung DV, Nga NT, Hoa LK (2017) Nonlinear stability of functionally graded material (FGM) sandwich cylindrical shells reinforced by FGM stiffeners in thermal environment. Applied Mathematics and Mechanics. 38:647–670. https://doi.org/10.1007/s10483-017-2198-9

Ghannad M, Rahim GH, Nejad MZ (2019) Elastic analysis of pressurized thick cylindrical shells with variable thickness made of functionally graded materials. Compos Part B Eng 45(1):388–396. https://doi.org/10.1016/j.compositesb.2012.09.043

Haddadpour H, Mahmoudkhani S, Navazi HM (2007) Free vibration analysis of functionally graded cylindrical shells including thermal effects. Thin-walled Struct 45:591–599. https://doi.org/10.1016/j.tws.2007.04.007

Han Y, Zhu X, Li T, Yu Y, Hu X (2018) Free vibration and elastic critical load of functionally graded material thin cylindrical shells under internal pressure. Int J Struct Stab Dyn 18(11):1850138. https://doi.org/10.1142/S0219455418501389

Huang H, Han Q (2008) Buckling of imperfect functionally graded cylindrical shells under axial compression. Eur J Mech A/Solids 27:1026–1036. https://doi.org/10.1016/j.euromechsol.2008.01.004

HuangHan HQ (2010) Nonlinear dynamic buckling of functionally graded cylindrical shells subjected to time-dependent axial load. Compos Struct 92:593–598. https://doi.org/10.1016/j.compstruct.2009.09.011

HuangHan HQ (2010) Research on nonlinear postbuckling of functionally graded cylindrical shells under radial loads. Compos Struct 92:1352–1357. https://doi.org/10.1016/j.compstruct.2009.11.016

Jabbari M, Nejad ZM, Ghannad M (2016) Thermo elastic analysis of axially functionally graded rotating thick truncated conical shells with varying thickness. Compos Part B-Eng 96:20–34. https://doi.org/10.1016/j.compositesb.2016.04.026

Kashkoli MD, Tahan KN, Nejad MZ (2018) Thermo-mechanical creep analysis of FGM thick cylindrical pressure vessels with variable thickness. Int J Appl Mech 10(1):1850008. https://doi.org/10.1142/S1758825118500084

Loy CT, Lam KY, Reddy JN (1999) Vibration of functionally graded cylindrical shells. Int J Mech Sci 41:309–324. https://doi.org/10.1016/S0020-7403(98)00054-X

Malekzadeh P, Heydarpour Y (2013) Free vibration analysis of rotating functionally graded truncated conical shells. Compos Struct 97:176–188. https://doi.org/10.1016/j.compstruct.2014.06.023

Matsunaga H (2009) Free vibration and stability of functionally graded circular cylindrical shells according to 2D higher-order deformation theory. Compos Struct 88:519–531

Nam VH, Phuong NT, Trung NT (2019) Nonlinear buckling and postbuckling of sandwich FGM cylindrical shells reinforced by spiral stiffeners under torsion loads in thermal environment. Acta Mech 230:3183–3204. https://doi.org/10.1007/s00707-019-02452-5

Nejad ZM, JabbariGhannad MM (2015) Thermo-elastic analysis of axially functionally graded rotating thick cylindrical pressure vessels with variable thickness under mechanical loading. Int J Eng Sci 96:1–18. https://doi.org/10.1016/j.ijengsci.2015.07.005

Nejad ZM, Jabbari M, Ghannad M (2017) A general disk form formulation for thermo-elastic analysis of functionally graded thick shells of revolution with arbitrary curvature and variable thickness. Acta Mechanica. 228(1):215–231. https://doi.org/10.1007/s00707-016-1709-z

Phu KV, Bich DH, Doan LX (2017) Analysis of nonlinear thermal dynamic responses of sandwich functionally graded cylindrical shells containing fluid. J Sandwich Struct Mater 21(6):1953–1974. https://doi.org/10.1177/1099636217737235

Phu KV, Bich DH, Doan LX (2019) Nonlinear thermal vibration and dynamic buckling of eccentrically stiffened sandwich-FGM cylindrical shells containing fluid. J Reinf Plast Compos 38(6):253–266. https://doi.org/10.1177/0731684418814636

Pradhan SC, Loy CT, Lam KY, Reddy JN (2000) Vibration characteristics of functionally graded cylindrical shells under various boundary conditions. Appl Acoust 61:111–129. https://doi.org/10.1016/S0003-682X(99)00063-8

Quan TQ, Duc ND (2016) Nonlinear vibration and dynamic response of shear deformable imperfect functionally graded double-curved shallow shells resting on elastic foundations in thermal environments. J Therm Stresses 39(4):437–459. https://doi.org/10.1080/01495739.2016.1158601

Quan TQ, Phuong T, Tuan ND, Duc ND (2015) Nonlinear dynamic analysis and vibration of shear deformable eccentrically stiffened S-FGM cylindrical panels with metal-ceramic-metal layers resting on elastic foundations. J Compos Struct 126:16–33. https://doi.org/10.1016/j.compstruct.2015.02.056

Selah E, Setoodeh AR, Tahani M (2014) Three-dimensional transient analysis of functionally graded truncated conical shells with variable thickness subjected to an asymmetric dynamic pressure. Int J Press Vessels Pip 119:29–38. https://doi.org/10.1016/j.ijpvp.2014.02.003

Shariyat M, Alipour MM (2017) Analytical bending and stress analysis of variable thickness FGM auxetic conical/cylindrical shells with general tractions. Lat Am J Solids Struct 14(5):805–843. https://doi.org/10.1590/1679-78253413

Shariyat M, Asgari D (2013) Nonlinear thermal buckling and postbuckling analyses of imperfect variable thickness temperature-dependent bidirectional functionally graded cylindrical shells. Int J Press Vessels Pip 111–112:310–320. https://doi.org/10.1016/j.ijpvp.2013.09.005

Sofiyev AH (2003) Dynamic buckling of functionally graded cylindrical shells under non-periodic impulsive loading. Acta Mech 165(3–4):151–163. https://doi.org/10.1007/s00707-003-0028-3

Thanh NV, Quang VD, Khoa ND, Eock KS, Duc ND (2019) Nonlinear dynamic response and vibration of FG CNTRC shear deformable circular cylindrical shell with temperature-dependent material properties and surrounded on elastic foundations. J Sandwich Struct Mater 21(7):2456–2483. https://doi.org/10.1177/1099636217752243

Volmir AS (1972) Nonlinear dynamics of plates and shells. Science Edition, Moscow

Wann KY (2015) Free vibration analysis of FGM cylindrical shell partially resting on Pasternak elastic foundation with an oblique edge. Compos B Eng 70:263–276. https://doi.org/10.1016/j.compositesb.2014.11.024

Zhang J, Chen S, Zheng W (2019) Dynamic buckling analysis of functionally graded material cylindrical shells under thermal shock. Continuum Mech Thermodyn 32:1095–1108. https://doi.org/10.1007/s00161-019-00812-z